X-723-69-251
PREPRINT

NASA TM X-63764

RAE ANTENNA-DAMPER PACKAGE DEPLOYMENT INTERACTION

JOSEPH V. FEDOR
BOWDEN W. WARD, JR.

JULY 1969

GSFC

GODDARD SPACE FLIGHT CENTER
GREENBELT, MARYLAND

X-723-69-251

RAE ANTENNA-DAMPER PACKAGE DEPLOYMENT INTERACTION

Joseph V. Fedor
Bowden W. Ward, Jr.

July 1969

Goddard Space Flight Center
Greenbelt, Maryland

PRECEDING PAGE BLANK NOT FILMED.

CONTENTS

ILLUSTRATIONS

PRECEDING PAGE BLANK NOT FILMED.

RAE ANTENNA-DAMPER PACKAGE DEPLOYMENT INTERACTION

INTRODUCTION

During the planning of the deployment sequence of the Radio Astronomy Explorer, a gravity gradient stabilized spacecraft, a question arose as to when to deploy the libration damper package. The damper package is normally housed internal to the spacecraft and sometime during the spacecraft deployment phase, the package must be extended externally. The 24.5 pound package is accelerated by four one-pound negator springs to 2.3 ft/sec in traversing approximately 12 inches from inside to outside the spacecraft and then is stopped abruptly. Two deployment times or methods were considered: the first was to deploy the package prior to main boom deployment, during magnetic stabilization and the other was after main boom deployment. Thermal and dynamic effects tended to constrain the first method, while the effect of damper package shock motion on the main booms constrained the other method. This analysis addresses itself to assessing the effect of deploying the damper package after main boom deployment.

PROBLEM STATEMENT

The orbital configuration of the RAE spacecraft with the "V" antennas deployed to an intermediate length of 450 ft is illustrated in Figure 1.

Antenna deflections due to gravity and other orbital environment effects are neglected in this analysis. Since the deflections due to these effects are in the linear range, they can be added in a superposition fashion if desired. A free body diagram of a portion of one of the antennas is shown in Figure 2. The reaction acceleration, a_3, experienced by the antenna boom during and after damper package deployment is resolved into components parallel and transverse to the antenna direction. This analysis considers the bending effect of the transverse loading but does not consider tension-compression effects which may result because of the parallel component of loading. The basic problem is to solve for the antenna deflection by adding the transverse loading terms due to the various accelerations to the standard <u>linearized</u> equation of beam bending:

$$\frac{\partial^4 y}{\partial x^4} = \frac{\text{acceleration loading per unit length}}{EI} \tag{1}$$

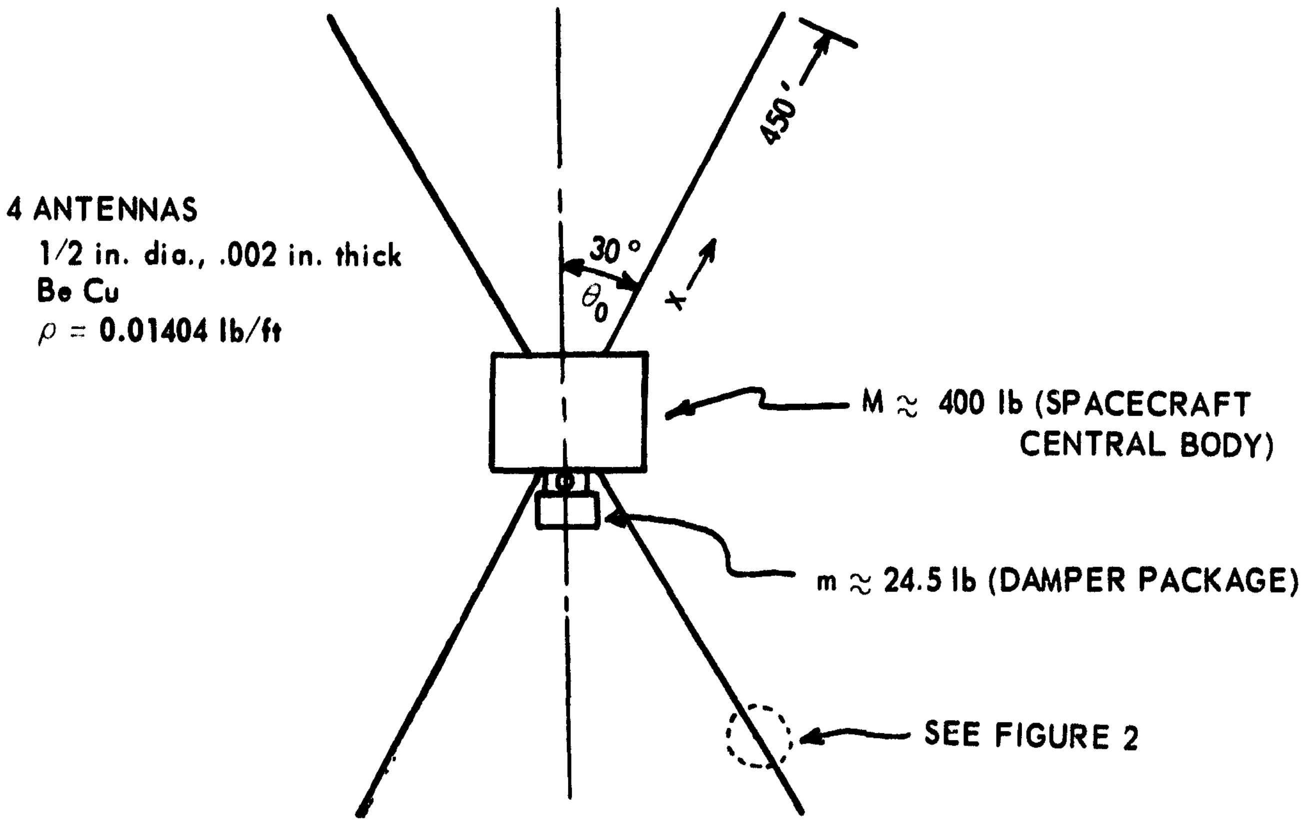

Figure 1–RAE Deployed Configuration

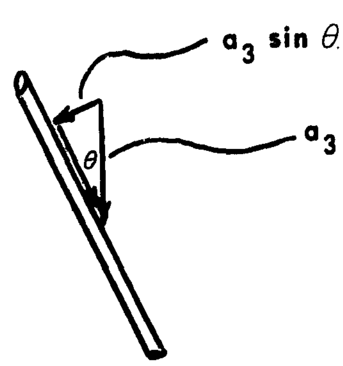

Figure 2–Resolution of Reaction Acceleration into Parallel and Normal Components

where

x = distance along the axis of an undeformed antenna, ft (local coordinate system)

y = deflection perpendicular to the undeformed antenna axis, ft

EI = flexural rigidity, lb-ft^2

The local coordinate system is embedded in the hub of the spacecraft and the hub is considered as a mass point.

The acceleration loading consisted of three parts:

1. That due to motion of antenna element with respect to local coordinate system: $\partial^2 y / \partial t^2$

2. That due to linear motion of hub and hence local coordinate system as antennas deflect: $\partial^2 \xi / \partial t^2$

3. That due to rigid body reaction motion of main spacecraft because of damper package deployment: a_3

The first acceleration term, $\partial^2 y / \partial t^2$, is self evident and needs no further explanation. The displacement of the hub, ξ, and hence $\partial^2 \xi / \partial t^2$ can be expressed in terms of antenna deflection by using the principle of first mass moment. Referring to Figure 3, the first mass moment of the upper and lower antennas respectively is

Upper V $$2 \int_0^{\ell} \eta_1 \rho \, d s \tag{2a}$$

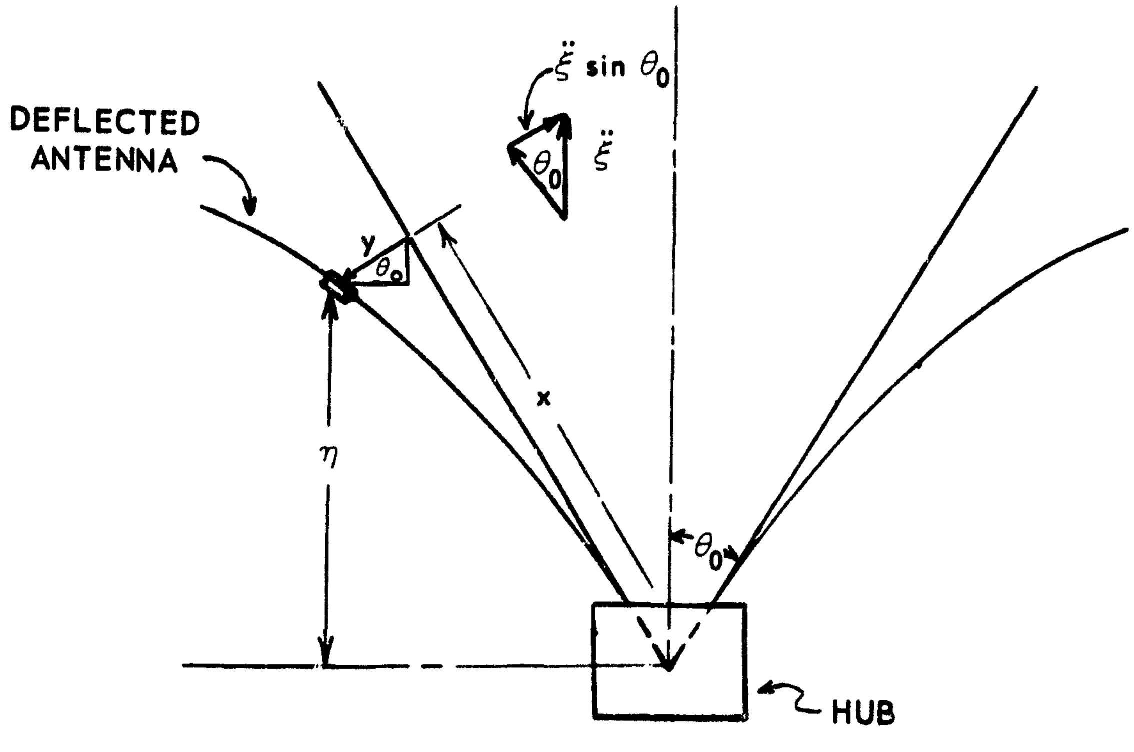

Figure 3–Antenna Coordinate System

where

$$\eta_1 = x \cos \theta_0 - y \sin \theta_0 \tag{2b}$$

and

Lower V

$$2 \int_0^{\ell} \eta_2 \, \rho \, ds \tag{2c}$$

where

$$\eta_2 = x \cos \theta_0 + y \sin \theta_0 \tag{2d}$$

and s is a dummy variable of integration for x. Taking the difference and equating this to the product of total mass of spacecraft, M_T, and center of mass, ξ, we obtain

$$M_T \, \xi = -4 \rho \sin \theta_0 \int_0^{\ell} y(s, t) \, ds$$

or

$$\xi = -4 \rho \frac{\sin \theta_0}{M_T} \int_0^{\ell} y(s, t) \, ds \tag{3}$$

The acceleration is obtained by differentiation with respect to time twice

$$\frac{\partial^2 \xi}{\partial t^2} = - \frac{4 \rho \sin \theta_0}{M_T} \int_0^{\ell} \frac{\partial^2 y}{\partial t^2} (s, t) \, ds \tag{4}$$

Now the third acceleration term, a_3, was determined experimentally together with Newton's law of action and reaction as described in the next section of this report.

EXPERIMENTAL DETERMINATION OF a_3

In obtaining a_3 as a function of time a deployment test of the damper package was made under simulated zero-gravity conditions. The test gave the acceleration experienced by the damper package. By an application of Newton's third law, the reaction acceleration experienced by the rigid spacecraft hub and hence the booms is obtained. A schematic representation of the damper package as contained within the spacecraft is shown in Figure 4. There is a torsion wire supporting frame weighing approximately 3 lb which is driven downward in a track upon release until hard stops are reached. This occurs after a total travel of 12-3/8" at which time detents snap in place preventing back travel. Attached to this supporting frame through 4 shock absorbing springs (K = 70 lb/in.) is the main damper boom package weighing 21.5 lbs. This part of the damper package is free of its four teflon guide channels after about 4 inches of travel.

The complete package assembly is driven by four negator springs of approximately 1 lb force each. A maximum velocity of 2.3 ft/sec and a kinetic energy of 23.8 in.-lb are obtained by the time of impact with the hard stops. The four shock absorber springs absorb 11.4 in.-lb of the 21 in.-lb contained in the main damper package by compressing .213" at which time they are bottomed. A rebound then begins which results in a reverse acceleration being applied. The force is applied to the detent pawls which are locked into place in the spacecraft structure. No shock absorption is provided in this direction so a hard rebound occurs here. All these phenomena are observed and recorded by an accelerometer mounted on the main damper package.

An actual trace of the accelerometer output in g's during a simulated damper package deployment is shown in Figure 5a. After an initial constant acceleration and then a deceleration pulse, the shock deceleration damps out completely in

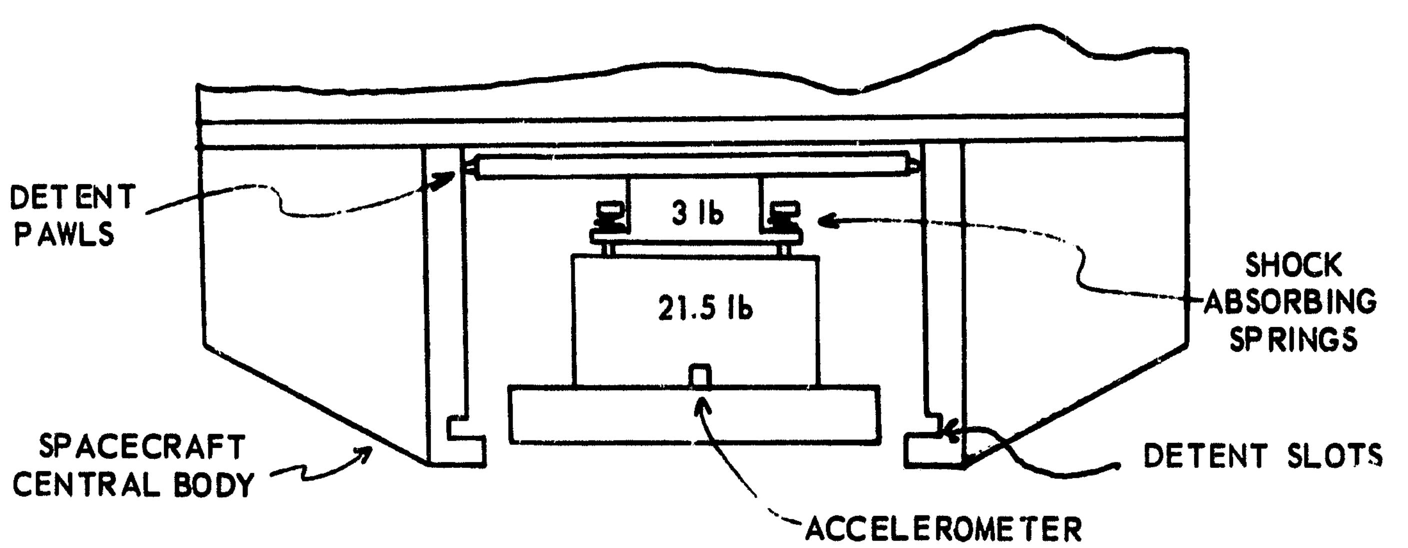

Figure 4–Damper Package in the Stowed Position within the Spacecraft

approximately 1.5 seconds so only the initial and final portions of the curve are shown. In Figures 5b, 5c, and 5d, enlarged views of the initial portion of the curve and modifications performed upon it to get it into a form more suitable for analytical treatment are shown. In addition, brief explanations of the steps taken to simplify the curve are given.

The final form is represented analytically in two parts: the first part by a constant acceleration term and the second part by the product of an initial acceleration, an exponential decay function, and the sine of transient frequency times time. These parts are:

$$a = \text{constant} \qquad 0 < t < \tau \tag{5a}$$

$$a = a_o\, e^{-\lambda t} \sin \Omega t \qquad \tau \leq t < \infty \tag{5b}$$

From Newton's third law of action and reaction

$$a_3 = -\frac{m}{M} a \tag{6}$$

where m is the mass of the damper package and M is the mass of the spacecraft less damper package. Thus, when all of the acceleration loading terms are included in Equation 1, the governing differential equation for each antenna is of the form

$$\frac{\partial^4 y}{\partial x^4} = -\frac{\rho}{EI}\frac{\partial^2 y}{\partial t^2} + \frac{4\rho^2 \sin^2\theta_0}{EIM_T}\int_0^{\ell}\frac{\partial^2 y(s,t)\,ds}{\partial t^2} + \frac{\rho a_3 \sin\theta_0}{EI} \tag{7}$$

where

$$a_3 = \frac{m a_0\, \Omega}{M\tau(\lambda^2 + \Omega^2)} \qquad 0 < t < \tau$$

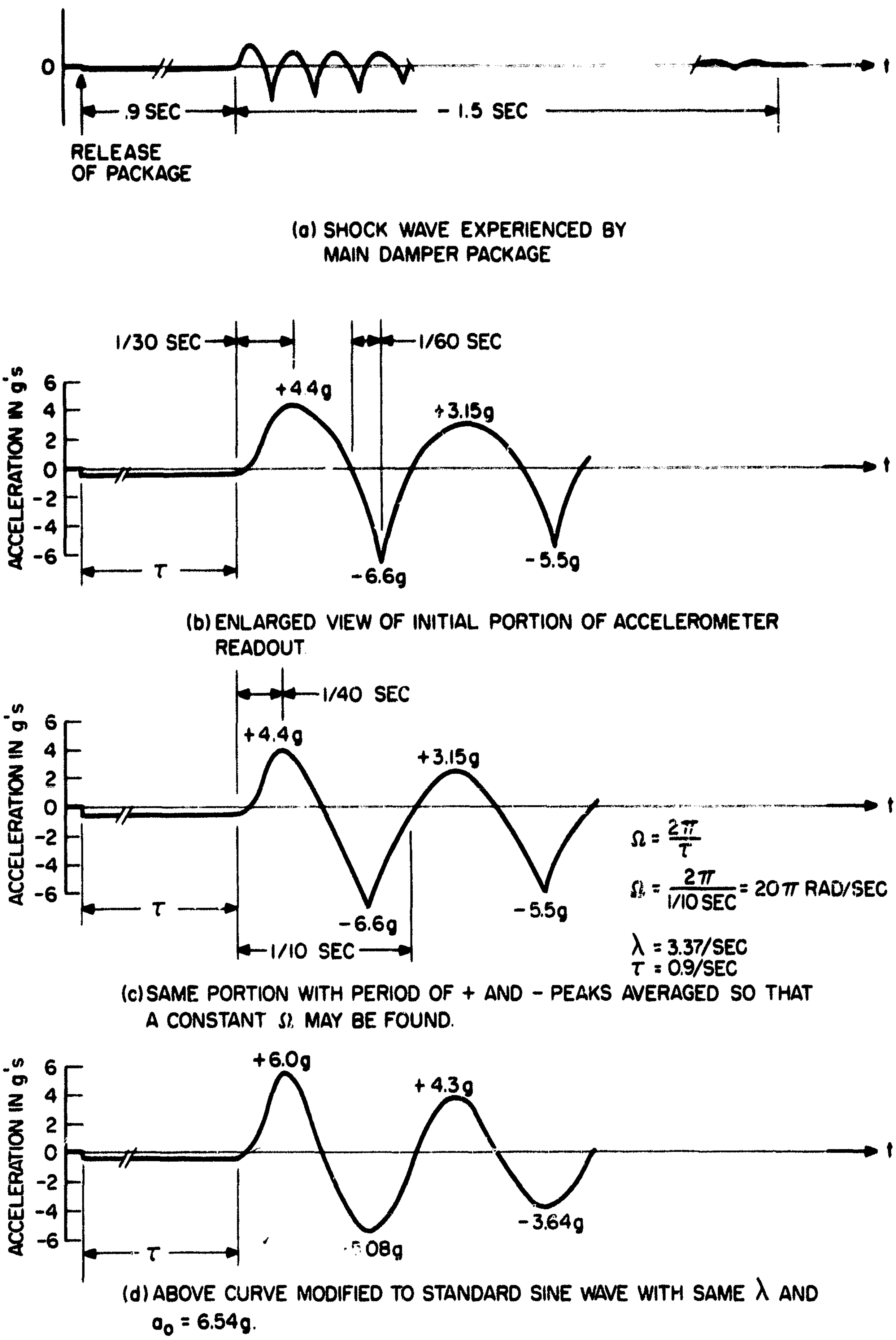

Figure 5–Modification of the Transient Disturbance Wave for Analytical Treatment

and

$$a_3 = -\frac{m}{M} a_0 e^{-\lambda(t-\tau)} \sin \Omega(t-\tau) \qquad \tau \le t < \infty$$

The amplitude of the first pulse was adjusted so that the integral of the acceleration ($\int_0^\infty a_3 \, dt$) is zero. This is a necessary condition so that no net velocity is imparted to the spacecraft due to the extension of the damper package.

The boundary conditions are:

$$y(0,t) = \frac{\partial y}{\partial x}(0,t) = 0 \qquad (8a)$$

$$\frac{\partial^2 y(\ell,t)}{\partial x^2} = \frac{\partial^3 y(\ell,t)}{\partial x^3} = 0 \qquad (8b)$$

and at t = 0

$$y(x,0) = \frac{\partial y}{\partial t}(x,0) = 0 \qquad (8c)$$

Equation 8a requires that the deflection and slope be zero at the origin. Equation 8b requires that the moment and shear be zero at the end of the antenna and Equation 8c requires that the antenna be quiescent at t = 0.

Equations 7 through 8c is an idealized dymanic statement of the antenna-damper package interaction. It is so formulated that only translation in the plane of the antennas is permitted to take place. Any rotational motion of the spacecraft hub due to misaligned deployment of the package is neglected. The governing differential equation will now be solved satisfying the specified boundary conditions and thus the deflection of a particular antenna and the resulting spacecraft configuration change will be determined.

SOLUTION OF GOVERNING DIFFERENTIAL EQUATION

The solution to Equation 7 can be facilitated by expanding unity in terms of cantilever mode shapes X_n (x) which satisfy the boundary conditions in Equations 8a, 8b and are solutions of the fourth order differential equation:

$$\frac{d^4 X_n}{dx^4} = \beta_n^4 X_n \tag{9}$$

The X_n (x) are dimensionless and normalized such that $X_n(\ell) = 1$, and β_n are the eigenvalues for the simple cantilever boundary conditions (see references 1, 3). It is well known that the set of X_n (x) form an orthonormal vector basis such that an arbitrary function can be expanded in terms of these quantities. (See reference 1.) Hence,

$$1 = \sum_1^\infty C_n X_n(x) \tag{10}$$

where the constants C_n are given by the usual integration procedure

$$C_n = \frac{\int_0^\ell X_n(x)\, dx}{\int_0^\ell X_n^2(x)\, dx} = \frac{4}{\ell} \int_0^\ell X_n(x)\, dx \tag{11a}$$

Equation 11a can be evaluated by using Equation 9. Thus,

$$\int_0^\ell X_n(x)\, dx = \frac{1}{\beta_n^4} \int_0^\ell X_n^{IV}(x)\, dx = \frac{X_n'''(x)}{\beta_n^4} \Bigg]_0^\ell$$

or (11b)

$$\int_0^\ell X_n(x)\, dx = - \frac{X_n'''(0)}{\beta_n^4}$$

since there is no shear at the end of the antenna. Explicitly, the C_n is given by

$$C_n = -\frac{4}{\ell}\frac{X_n''(0)}{\beta_n^4} \tag{12}$$

Equation 12 can be evaluated using tables given in reference 3. Substituting Equation 10 into Equation 7 results in the following

$$\frac{\partial^4 y}{\partial x^4} + \frac{\rho}{EI}\frac{\partial^2 y}{\partial t^2} = \left(\frac{4\rho^2 \sin^2\theta_0}{EIM_T}\int_0^\ell \frac{\partial^2 y}{\partial t^2}(s,t)\,ds + \frac{\rho\, a_3 \sin\theta_0}{EI}\right)\sum_1^\infty C_n X_n(x) \tag{13}$$

Suppose we let the antenna deflection, y (x,t), have the following form

$$y(x,t) = \sum_1^\infty A_n(t)\,X_n(x) \tag{14}$$

where the A_n (t) which are functions only of t and have the dimension of length are to be determined. Substituting Equation 14 into 13 and rearranging results in

$$\sum_1^\infty \left(\ddot{A}_n + \frac{EI\beta_n^4}{\rho}A_n - \frac{4\rho\sin^2\theta_0}{M_T}C_n\int_0^\ell \frac{\partial^2 y(s,t)}{\partial t^2}\,ds - C_n a_3 \sin\theta_0\right)X_n(x) = 0 \tag{15}$$

Since each term in the parentheses is a function of time and the X_n (x) are linearly independent, the coefficient of each X_n (x) must be zero. Thus,

$$\ddot{A}_n + \omega_n^2 A_n - \frac{4\rho\sin^2\theta_0}{M_T}C_n\int_0^\ell \frac{\partial^2 y(s,t)}{\partial t^2}\,ds - C_n a_3 \sin\theta_0 = 0$$

$$n = 1, 2, 3 \cdots \tag{16}$$

where

$$\omega_n^2 = \frac{EI\beta_n^4}{\rho}$$

The integral in the above is evaluated by substituting Equation 14 into 16 and using Equation 11a, the definition of C_K :

$$\ddot{A}_n + \omega_n^2 A_n - \frac{\rho \ell \sin^2 \theta_0}{M_T} C_n \sum_1^{\infty} C_k \ddot{A}_k - C_n a_3 \sin \theta_0 = 0 \qquad (17)$$

The infinite series in Equation 17 complicates the determination of the A_n . To circumvent this difficulty, a one term approximate solution will be obtained. That is, attention will be focused only on the determination of A_1 . Calculations not including the series term in Equation 17 showed that the first term contributed 98% to the total deflection. With this approximation, the equation for A_1 is

$$\ddot{A}_1 + \omega_1^2 A_1 - \frac{\rho \ell \sin^2\theta_0}{M_T} C_1^2 \ddot{A}_1 - C_1 a_3 \sin \theta_0 = 0$$

or in more compact notation (18)

$$\ddot{A}_1 + \omega^2 A_1 = Ba_3$$

where

$$\omega^2 = \frac{\omega_1^2}{\left(1 - \frac{\rho \ell \sin^2\theta_0}{M_T} C_1^2\right)} \qquad (19)$$

and

$$B = \frac{\sin\theta_0 C_1}{\left(1 - \frac{\rho \ell \sin^2\theta_0}{M_T} C_1^2\right)} \tag{20}$$

The denominator of Equations 19 and 20 indicates that $\rho\ell \sin^2\theta_0 C_1^2 / M_T$ must be much less than 1 for the approximation to be valid. Also, it will be noted that the natural frequency of the antenna system will be somewhat higher than the simple cantilever frequency. This is to be expected since the antenna system is tending toward a free-free beam frequency which is higher. For $0 \leq t < \tau$ the solution for A_1 (t) satisfying the initial conditions: $A_1(0) = \dot{A}_1(0) = 0$ (obtained from Equations 8c and 14) is

$$A_1(t) = \frac{B_1}{\omega^2}(1 - \cos\omega t) \tag{21}$$

where

$$B_1 = \frac{m a_0 \Omega B}{M\tau(\Omega^2 + \lambda^2)}$$

For $\tau \leq t < \infty$ the solution for $A_1(t)$ is

$$A_1(t) = \frac{B_1}{\omega^2}\sin\omega\tau \sin\omega(t-\tau) + \frac{B_1}{\omega^2}(1 - \cos\omega\tau)\cos\omega(t-\tau)$$

$$- G_2 \cos\omega(t-\tau) + \left(\frac{\lambda G_2}{\omega} - \frac{\Omega G_1}{\omega}\right)\sin\omega(t-\tau) \tag{22}$$

$$+ G_1 e^{-\lambda(t-\tau)}\sin\Omega(t-\tau) + G_2 e^{-\lambda(t-\tau)}\cos\Omega(t-\tau)$$

where

$$G_1 = \frac{(\lambda^2 + \omega^2 - \Omega^2)B_2}{[(\lambda^2 + \omega^2 - \Omega^2)^2 + 4\lambda^2\Omega^2]} \tag{23}$$

$$G_2 = \frac{2\lambda\Omega B_2}{[(\lambda^2 + \omega^2 - \Omega^2)^2 + 4\lambda^2\Omega^2]} \tag{24}$$

where

$$B_2 = \frac{ma_0B}{M}$$

It will be noticed that at $t = \tau$ both solutions give the same value for $A_1(\tau)$ and $\dot{A}_1(\tau)$ as they should. Further, it will be noticed that the exponential terms in Equation 22 rapidly damp out in a few seconds and so the deflection for the antenna several seconds after libration damper package deployment is essentially given by

$$A_1(t) = \left(\frac{B_1}{\omega^2}\sin\omega\tau + \frac{\lambda G_2}{\omega} - \frac{\Omega G_1}{\omega}\right)\sin\omega(t-\tau)$$

$$+ \left(\frac{B_1}{\omega^2}(1-\cos\omega\tau) - G_2\right)\cos\omega(t-\tau) \tag{25}$$

$$t >> \tau$$

For $w\tau$ small (which is true for RAE parameters). Equation 25 simplifies to

$$A_1(t) = \left(\frac{B_1\tau}{\omega} + \frac{\lambda G_2}{\omega} - \frac{\Omega G_1}{\omega}\right)\sin\omega(t-\tau)$$

$$+ \left(\frac{B_1\tau^2}{2} - G_2\right)\cos\omega(t-\tau) \tag{26}$$

Consistent with the one term approximation and the normalization discussed earlier, the tip deflection is determined by setting $x = \ell$ in Equation 14

$$y(\ell, t) = A_1(t)X_1(\ell) = A_1(t) \tag{27}$$

The hub movement is obtained from the following formula

$$\xi = -\frac{\rho \ell \sin \theta_0 C_1 A_1(t)}{M_T} \tag{29}$$

which was derived from Equation 3. Another quantity of interest is the root moment acting on the antenna. This is given by the usual beam formula

$$\text{Moment} = EI \frac{\partial^2 y}{\partial x^2} = EI A_1(t)\ X_1''(0) \tag{28a}$$

$$= EI\ \beta_1^2\ A_1(t) \tag{28b}$$

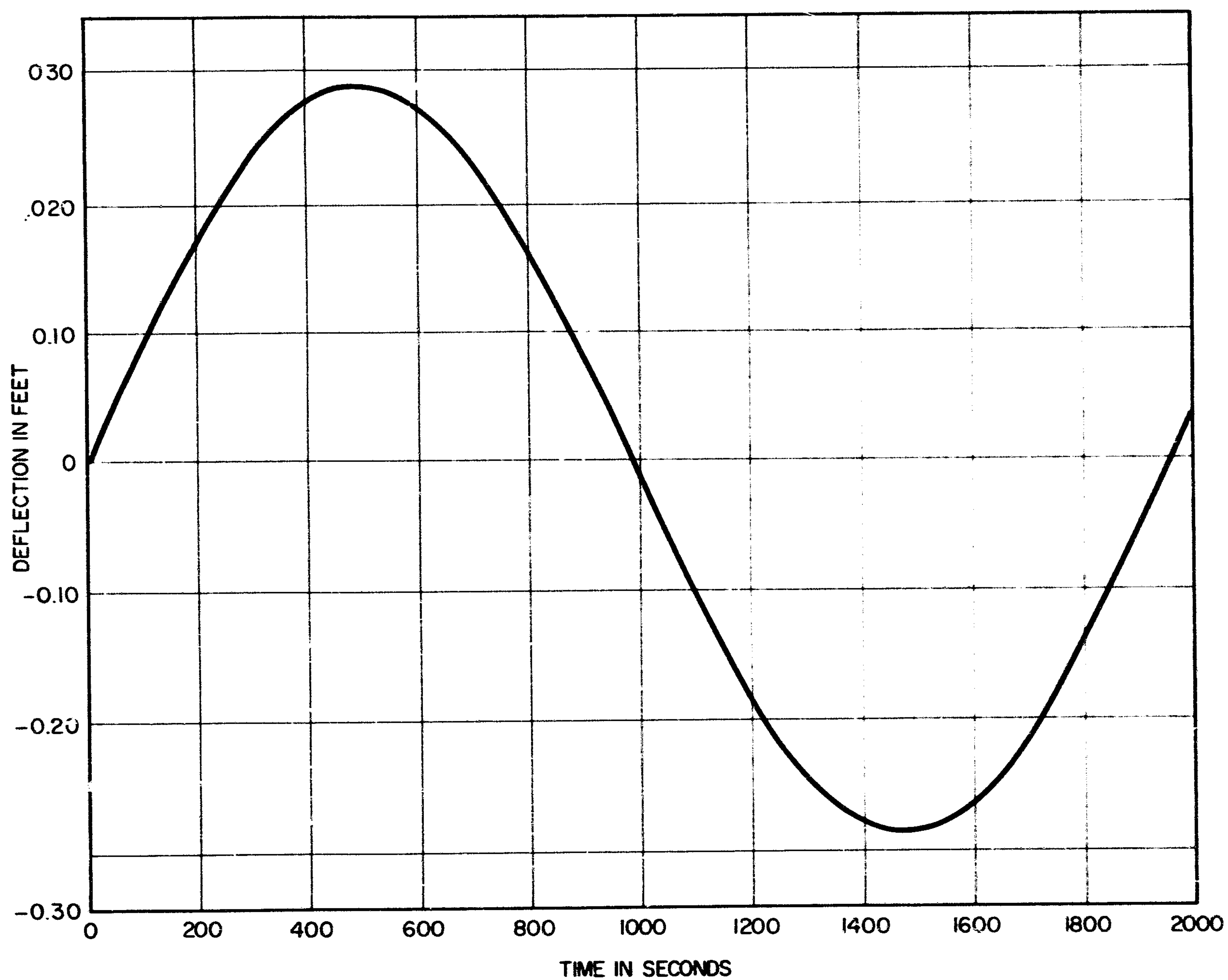

Figure 6–Antenna Tip Deflection Following Damper Package Deployment

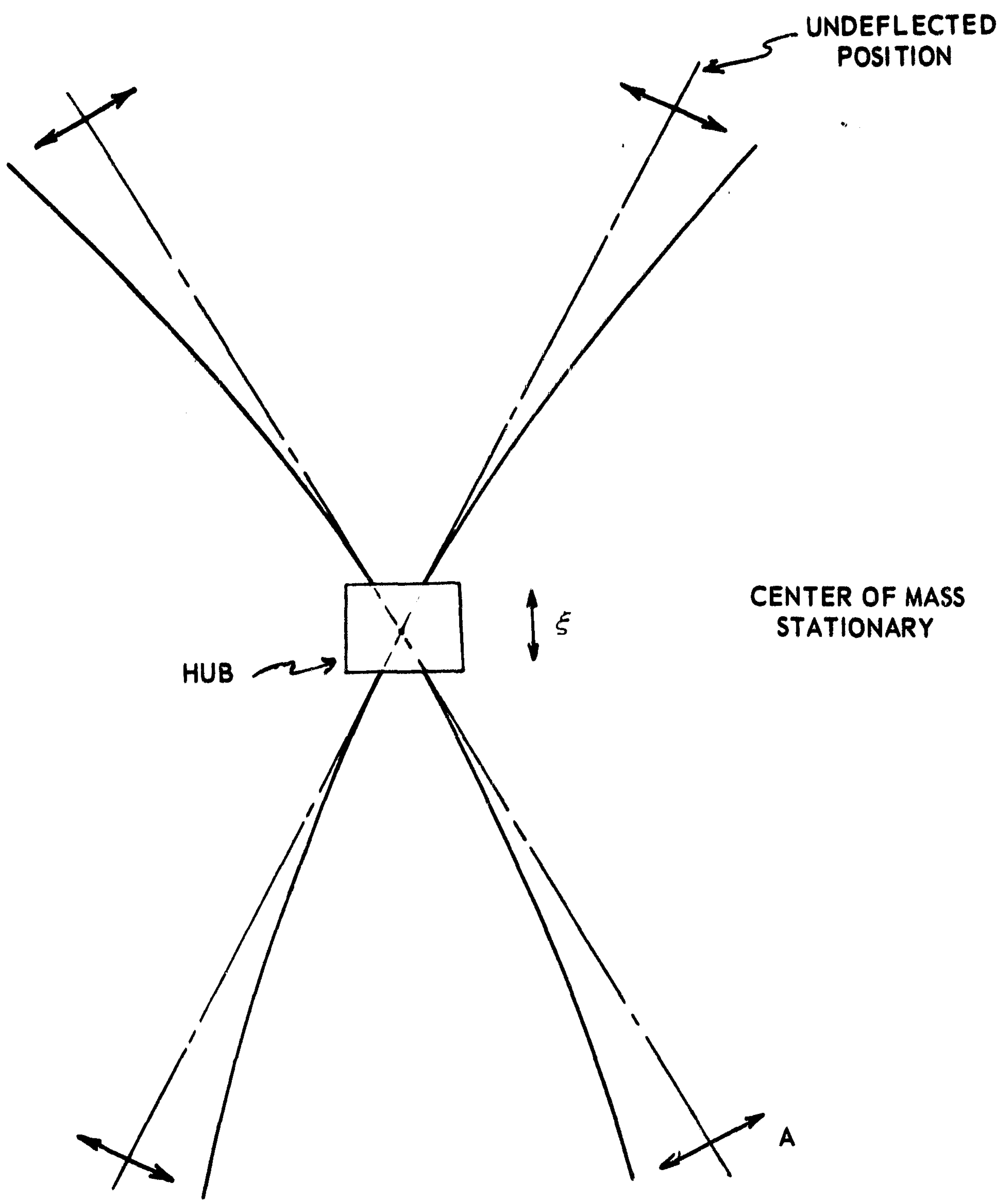

Figure 7–Motion of Spacecraft Following Damper Package Deployment. The deflections shown are highly exaggerated for illustrative purposes.

DISCUSSION OF RESULTS

Figure 6 shows a plot of antenna deflection versus time using the one term approximate solution. The numerical values of the physical parameters used are given in Appendix A. The salient points of the plot are, that maximum antenna deflection occurs 8 minutes after damper package deployment, and the maximum value is approximately 0.29 feet. The relatively long time to peak deflection is due to the inherently slow response of the long antenna element. The small deflection is due to the cancelling pulses of the damper package first accelerating and then decelerating. This can be seen by noting that for the RAE spacecraft, Ω is much larger than λ and ω. With this approximation, G_1 and G_2 can be simplified to

$$G_1 = \frac{(\lambda^2 + \omega^2 - \Omega^2) B_2}{[(\lambda^2 + \omega^2 - \Omega^2)^2 + 4\lambda^2\Omega^2]} \approx - \frac{B_2}{\Omega^2 + 3\lambda^2} \tag{30}$$

$$G_2 = \frac{2\lambda\Omega B_2}{[(\lambda^2 + \omega^2 - \Omega^2)^2 + 4\lambda^2\Omega^2]} \approx \frac{2\lambda B_2}{\Omega(\Omega^2 + 2\lambda^2)} \tag{31}$$

where terms the order of λ^2/Ω^2 have been neglected compared to 1. Substituting Equations 30 and 31 into Equation 26 and retaining terms the order of $1/\omega\Omega$ results in the following expression for $A_1(t)$:

$$A_1(t) = \frac{a_0 m B \Omega}{M\omega}\left(\frac{1}{\Omega^2 + \lambda^2} - \frac{1}{\Omega^2 + 3\lambda^2}\right) \sin \omega(t - \tau) \tag{32a}$$

or

$$A_1(t) = \frac{2a_0 m B \Omega \lambda^2 \sin \omega(t - \tau)}{M\omega(\Omega^2 + \lambda^2)(\Omega^2 + 3\lambda^2)} \tag{32b}$$

where

$$B = \frac{\sin \theta_0 C_1}{\left(1 - \frac{\rho \ell}{M_T} \sin^2 \theta_0 C_1^2\right)}$$

The "bucking" terms are seen in Equation 32a and the net result is given in Equation 32b. Figure 7 shows the resulting changes of spacecraft configuration due to the deflections given by Equation 32b. Essentially the upper pair of antennas move outward while the lower pair move inward and vice versa in a sinusoidal fashion long after the applied transient load becomes small. This motion is one of the normal modes of vibration of the spacecraft identified in reference 2. As was noted in the analysis, the antenna motion causes the hub of the spacecraft to move up and down about the equilibrium. Because of the small antenna deflections, the hub motion is small as well as the bending moment at the root of the antenna.

Of concern during the RAE Program was the antenna deflection and whether the antenna motion damps out after a period of time. The vibration mode excited by the damper package deployment was used to initialize the RAE dynamics simulator and it was found that the antenna motion did not damp out but persisted indefinitely. This showed that the libration damper would not take out this type of antenna motion even if it was made functional a short time after deployment.

There was apprehension as to how the RAE long antennas would behave in an orbital environment. A preliminary analysis of the damper package deployment had indicated greater deflections of the long antennas than the results presented herein which were not complete at the time of finalizing the launch sequence. Because of the desirability of adhering to conservative approaches, it was decided to deploy the damper package prior to deploying the long antennas.

In the actual flight of the RAE-A Spacecraft, the damper package was deployed successfully in this manner.

REFERENCES

1. S. Timoshenko, "Vibration Problems in Engineering," pp.331-336, D. Van Nostrand Company, Inc., Publisher.

2. Newton, J. K. and Farrell, J. L., "Natural Frequencies of a Flexible Gravity Gradient Satellite," AIAA Journal of Spacecraft and Rockets, Vol. 5, No. 5 May 1968, pp. 560-569.

3. Young, Dana and Felgar, R. P., "Tables of Characteristic Functions Representing Normal Modes of Vibration of a Beam," The University of Texas Publication No. 4913, July 1949.

APPENDIX A
NUMERICAL CALCULATIONS

I. ANTENNA DEFLECTION

Initial Values of Parameters

$\Omega = 20\pi$ rad/sec

$\wedge = 3.37\ \text{sec}^{-1}$

$a_0 = 6.54$ g

m = 24.5 lb

M = 400 lb

$M_T = 424.5$ lb

EI = 2,130 lb in.^2

$\rho = 1.1697 \times 10^{-3}$ lb/in. or 3.03×10^{-6} lb $\text{sec}^2/\text{in.}^2$

$\theta_0 = 30°$

$g = 32.159\ \text{ft/sec}^2$

$\ell = 5400$ in.

$$\left.\begin{array}{l} \phi_1'''(0) = -1.46819 \\ \beta_1 \ell = 1.8751041 \end{array}\right\} \text{For Clamped-Free Beam (See Reference 3)}$$

$\tau = 0.9$ sec

Calculated Values

1.
$$\omega_1^2 = \frac{EI}{\rho}\beta_1^4$$

$$\omega_1^2 = \frac{2.13 \times 10^3}{3.03 \times 10^{-6}} \left(\frac{1.8751041}{5.4 \times 10^3}\right)^4$$

$$\omega_1 = 0.003196919 \text{ rad/sec}$$

2.

$$C_n = -\frac{4}{\ell} \frac{X_n'''(0)}{\beta_n^4}$$

or (12)*

$$C_n = -\frac{4}{\ell} \frac{\phi_n'''(0)}{2\beta_1}$$

upon substitution of $X_n = \phi_n/2$

$$C_1 = -\frac{4}{\ell}\left[\frac{-1.46819}{2\left(\frac{1.8751041}{\ell}\right)}\right]$$

$$C_1 = 1.565982$$

3.

$$\omega^2 = \frac{\omega_1^2}{\left(1 - \frac{\rho \ell \sin^2 \theta_0 C_1^2}{M_T}\right)}$$

$$\omega^2 = \frac{(0.003196919)^2}{\left(1 - \frac{(1.1697 \times 10^{-3})(5.4 \times 10^3)(.5)^2(1.565982)^2}{424.5}\right)} \tag{19}$$

$$\omega^2 = 1.031439 \times 10^{-5}$$

---

*Numbers refer to equations in the main text or

$$\alpha = 3.21602 \times 10^{-3}$$

4.

$$A_{1\,max} = \frac{2a_0 mB\Omega\lambda^2}{M\omega(\Omega^2 + \lambda^2)(\Omega^2 + 3\lambda^2)}$$

where

$$B = \frac{\sin\theta_0 C_1}{\left(1 - \frac{\rho \ell \sin^2\theta_0 C_1^2}{M_T}\right)}$$

$$B = \frac{0.5\,(1.565982)\,(32.159)}{\left(1 - \frac{(1.1697 \times 10^{-3})\,(5.4 \times 10^3)\,(.5)^2\,(1.565982)^2}{424.5}\right)}$$

$$B = 25.41202 \text{ ft/sec}^2$$

$$A_{1\,max} = \frac{2(6.54)(24.5)(25.41202)(20\pi)(3.37)^2}{400(3.21602 \times 10^{-3})((20\pi)^2 + (3.37)^2)((20\pi)^2 + 3(3.37)^2)}$$

$$A_{1\,max} = 0.286534 \text{ ft}$$

A plot of deflection versus time is shown in Figure 6. The first maximum value of 0.287 ft occurs when t = 489.3 seconds.